# A Zinc-Finger_Family Transcription Factor, *AbVf19*, is Required for the Induction of a Gene Subset Important for Virulence in *Alternaria brassicicola*

Akhil Srivastava[1], Robin A. Ohm[2], Lindsay Oxiles[1], Fred Brooks[1], Christopher B. Lawrence[3], Igor V. Grigoriev[2] and Yangrae Cho[1]

1. Plant and Environmental Protection Sciences, University of Hawaii at Manoa, 3190 Maile Way, St. John 317, Honolulu 96822, U.S.A.
2. United States Department of Energy Joint Genome Institute, 2800 Mitchell Drive, Walnut Creek, CA 94598, U.S.A.
3. Virginia Bioinformatics Institute and Department of Biological Sciences, Virginia Tech, Blacksburg 24061, U.S.A.

December 2011

The work conducted by the U.S. Department of Energy Joint Genome Institute is supported by the Office of Science of the U.S. Department of Energy under Contract No. DE-AC02-05CH11231

## DISCLAIMER

**Transcription factor *AbVf19* induces hydrolytic enzyme genes during pathogenesis in *Alternaria brassicicola***

**Running title:**

Akhil Srivastava[1], Robin A. Ohm[2], Lindsay Oxiles[1], and Fred Brooks[1], Igor V. Grigoriev[2], Yangrae Cho[1]*

[1] Plant and Environmental Protection Sciences, University of Hawaii at Manoa, 3190 Maile Way, St. John 317, Honolulu, HI 96822
[2] US Department of Energy Joint Genome Institute, 2800 Mitchell Drive, Walnut Creek, CA 94598

*Corresponding author
Yangrae Cho
Department of Plant and Environmental Protection Sciences
University of Hawaii at Manoa,
Honolulu, HI 96822
Tel: 1-808-956-5305
Fax: 1-808-956-2832
Email address: yangrae@hawaii.edu

*AbVf19* (*Alternaria brassicicola* virulence factor 19) GenBank accession number: JN835469
RNA-seq data: GSE33148

**ABSTRACT**

*Alternaria brassicicola* is a successful saprophyte and necrotrophic pathogen with a broad host range. It produces secondary metabolites that marginally affect virulence, in contrast to many *A. alternata* strains that produce secondary metabolites as host-specific pathogenicity factors. Cell wall-degrading enzymes (CWDEs) have been considered important for pathogenesis, but no CWDEs have been identified as significant virulence factors in *A. brassicicola*. In this study, we discovered mutants of a gene, *AbVf19*, which consistently produced smaller lesions than the wild type. The mutants grew slower than the wild type on an axenic medium with pectin as a major carbon source. Gene expression comparisons identified several hydrolytic enzyme-coding genes being down-regulated in the mutant during a late stage of infection. These down-regulated genes comprised a small fraction of genes within each family. Three of these genes had mutants that showed no or little change in virulence. This suggests that each down regulated gene only made a small contribution to virulence, or that their functions were redundant. This study demonstrates the existence and importance of a transcription factor that regulates a suite of genes that are probably important for decomposing and utilizing plant material during the late stage of plant infection.

## INTRODUCTION

*Alternaria brassicicola* is the causal agent of black spot disease of cultivated brassicas, such as cabbage, canola, and mustard. It has also been used in studies of host-pathogen interactions on *Arabidopsis*. Pathogenesis in necrotrophic fungi is generally described as a two-step process of initially killing host cells directly (necrosis) or inducing programmed cell death with toxins, followed by or in conjunction with decomposing tissues with cell wall-degrading enzymes (CWDEs).

The importance of toxins in disease development has been clearly demonstrated in other necrotrophic fungi (Churchill et al., 1995; Ciuffetti et al., 1997a; Del Sorbo et al., 2000; Yun et al., 1998). Several *A. alternata* pathotypes produce toxic, host-specific secondary metabolites that are pathogenicity factors (Ito et al., 2004; Johnson et al., 2000; Spassieva et al., 2002; Tanaka et al., 1999). Several secondary metabolites and proteins in *A. brassicicola* have been identified as toxins, such as depudecin (Wight et al., 2009), brassicenes (Hashimoto et al., 2009), Brassicicolin A (Pedras et al., 2009a), and two proteins (Oka et al., 2005; Otani et al., 1998). All toxins produced by *A. brassicicola*, however, are weak virulence factors that only marginally affect pathogenesis.

The importance of CWDE genes in virulence has been supported by identification of mutants with impaired derepression mechanisms of carbon catabolite repression in *Colletotrichum carbonum* and *Fusarium oxysporum* (Ospina-Giraldo et al., 2003; Tonukari et al., 2000). Mutation of the sucrose nonfermenting factor 1 (SNF1) homolog showed severely reduced virulence in these two fungi. It has been speculated that coordinated expression of many CWDE genes is needed for successful pathogenesis. In contrast, mutants of the homologous gene *AbSnf1*, and its downstream gene *AbCreA*, were as virulent as the wild type (Cho et al., 2009). These findings suggested that *A. brassicicola* uses a different regulatory mechanism for CWDE genes during pathogenesis.

In addition to the weak roles of secondary metabolites or protein toxins, no single CWDE was identified as important for pathogenesis in *A. brassicicola*. For example, inefficient utilization of xylan due to loss of the transcription factor regulating the xylanase gene did not affect virulence

(Cho et al 2009), nor did the individual removal of over 12 genes encoding predicted CWDEs (Cho unpublished data). Slow growth of a deletion mutant of the pathogenicity factor gene *AbSte12*, with pectin as a major carbon source, suggested that the gene was necessary for the induction of pectin digestion enzymes. Its upstream mitogen-activated protein (MAP) kinase gene, *Amk1*, was necessary for the induction of several hydrolytic enzyme-coding genes (Cho et al. 2007).

In addition to the loss of pathogenicity, deletion mutants of the *AbSte12* gene (Δ*abste12*) had reduced growth rates compared to the wild type and impaired conidium maturation. Mutants of the *Amk1* gene showed more severe phenotypes than those of Δ*abste12*. The highly pleiotropic nature of Δ*abste12* and *amk1* mutants made it difficult to interpret their mechanistic roles in pathogenesis. In this study, we identified mutants that exhibited severely reduced virulence but did not show additional developmental defects. Our study provides an example of a transcription factor gene that plays a critical role in regulating virulence by coordinated expression of a suite of genes, including putative CWDE genes, in the necrotrophic plant pathogen, *A. brassicicola.*

## RESULTS

### Disruption mutants of the *AbVf19* gene

We systematically created mutants for over 200 genes by a single homologous recombination-based gene disruption method described previously (Cho et al., 2006). During our pathogenicity assays of the knockout mutants, we discovered one gene whose mutants showed a 90% decrease in virulence. The disrupted gene was located at the end of the brassWGS_Contig379 in the *A. brassicicola* genome (http://jgi.doe.gov/Abrassicicola). A partial coding sequence was missing at the 5' side. The nucleotide sequence of an ~2 Kb (exact size determined by two primers) fragment was determined and identified the predicted start codon, an intergenic region, and an adjacent coding region. The gene of interest was predicted to encode 564 amino acids with nuclear localization signals (probability 95%) at two locations predicted by PSORT (Horton and Nakai, 1997) and two $C_2H_2$-zinc finger domains (Pfam ID: PF00096) (Bateman et al., 2004). Only one copy of the gene was present in the draft genome sequence of *A. brassicicola*.

The tandem putative DNA binding domains are highly conserved among fungi in the Ascomycota, including *Saccharomyces cereviciae* (Supplementary Fig.1). All ascomycete fungi in the Pezizomycotina with genome sequences publically available had a homolog in their genomes (Fig. 1). The overall sequence was 34% to 91% identical among Pezizomycotina. The gene was most closely related to the homolog in *Pyrenophora tritici*, with 494 of 567 (91%) identical amino acid sequences. A homolog in *Neurospora crassa* showed 205 of 606 (34%) identical amino acid sequence. The functions of its homolog were annotated in many cases as either a hypothetical protein or a predicted $C_2H_2$-transcription factor. In the genomes of most Eurotiomycetes and in the genome of *Trichoderma atroviride*, its homolog was annotated as a fungal STRE-element-binding protein (Seb1). This gene is involved in but not essential for the osmotic stress response in *T. atroviride* (Seidl et al., 2004). Its homolog was annotated as a cutinase G-box binding protein in four fungal genomes, including *Pyrenophora tritici-repentis* (Pt-1C-BFP), but without experimental evidence. We named this gene, *AbVf19* (*Alternaria brassicicola* virulence factor 19).

**Replacement of the *AbVf19* gene with a HygB cassette**

We created additional null mutants of *AbVf19* by replacing the coding region with a Hygromycin B transferase (Hyg B) gene cassette. Southern hybridization with three probes against the genomic DNA extracted from eleven transformants and purified by single-spore isolation confirmed that the *AbVf19* gene was absent from four of eleven transformants (Fig. 2). The *AbVf19* coding region was replaced by a single copy of the HygB resistance cassette in one mutant (*Δabvf19-1*) and by multiple copies in three gene-deletion mutants (*Δabvf19-8*, *Δabvf19-9*, and *Δabvf19-10*).

**Decreased virulence of the *Δabvf19* mutants on green cabbage**

We performed pathogenicity assays to further characterize virulence attributes associated with *AbVf19*. All four deletion mutants produced significantly smaller lesions ($p<0.001$) than the wild type in each assay using various concentrations of inoculum on detached leaves (Table 1). The mutants consistently produced smaller lesions at concentrations of 1,000 and 2,000 conidia compared to the wild type (Fig. 3 A). The relative reduction in virulence was slightly less with 2,000 conidia on detached leaves, however, so we used 2,000 conidia for the pathogenicity

assays on whole plants to compare the lesions produced by the wild type and *Δabvf19*. The lesion produced by *Δabvf19-1* was similarly reduced compared to the wild type on whole plants (Fig. 3 B). Because pathogenicity assay results on detached leaves and whole plants were comparable, we used detached leaf assays for speed and convenience with other strains of mutant. We also compared lesions produced by the wild type, *Δabvf19* mutant, and a mutant complemented with a wild type allele (*Δabvf19:AbVf19*). Lesions produced by the complemented mutant were similar to those produced by the wild type, while the *Δabvf19* mutant showed a severe reduction in virulence (Fig 3. C).

We performed additional inoculations with *Δabvf19-8* using spore concentrations up to 10,000 conidia. Wild-type spores produced progressively, although not exactly proportionally, larger lesions with increasing conidial concentrations. For example, 2,000 conidia caused lesions twice as large as 1,000 conidia (Fig. 3 A). The *Δabvf19* mutants, however, created similar-sized lesions at concentrations of 2,000, 5,000, and 10,000 conidia (Fig. 3 D). The lesions produced by 5,000 and 10,000 mutant conidia were still 74% and 62% smaller respectively than lesions produced by 2,000 wild-type conidia (Table 1). The mutant produced smaller lesions than the wild type on green cabbage (*Brassica oleracea*) even when the inoculum contained 20 times more conidia (data not shown).

**No difference in germination**

We compared germination of the *Δabvf19-1* mutant and the wild type on minimal medium agar and potato dextrose agar (PDA). Germination for both the mutant and wild type three hours after inoculation on the two types of media was ~100%. The length of germ tubes was highly variable within each group (wild type and mutant). The average difference in length between mutant and wild type germ tubes was not statistically significant on minimal medium agar or PDA, though the mutant germ tubes were slightly shorter than those of the wild types (Fig. 4 A).

Germination was slower on *B. oleracea* than on synthetic media for both the wild type and the *Δabvf19* mutant. Germination rates for both the wild type and mutant were about 50% at 12 hours post-inoculation (hpi) and 100% at 24 hpi (Fig. 5). Germ tube length on host plant leaves varied within each group but average length was similar most of the time between the two groups

at 12 hpi. A small swollen structure (appressorium-like structure thereafter) was formed in a similar frequency at the tip of germ tube produced by both mutant and wild type by 24 hpi (Figure 5).

**No special effects of stress on mutant growth**

To determine if *AbVf19* was an important gene in the pathogen's response to oxygen or osmotic stress, like its homolog Seb1 (Seidl et al., 2004), we measured hyphal growth on PDA plates in the presence of 2% and 4% NaCl, and in 1, 2, and 4mM $KO_2$. These chemicals affected the growth of both the wild type and mutant *A. brassicicola* equally (data not shown).

**Inefficient use of pectin by the mutant**

To determine the reason for reduced virulence in the mutant, fungal growth rates were compared in axenic broth media containing different carbon sources. We grew the mutants and wild type in a minimal medium broth supplemented with glucose as a major carbon source. Biomass, measured as dry mycelial weight, was similar for the mutant and the wild type (Fig. 4 B), suggesting that glucose did not affect vegetative growth of the mutant. Both Δ*abvf19* and wild type *A. brassicicola* grew very slow in the presence of α-cellulose or xylan as a major carbon source, thus we did not investigate their effect on mutant growth. Both the wild type and mutant produced almost 300% more mycelial biomass in glucose-yeast extract broth (GYEB) than in minimal media supplemented with glucose. The difference between the two was not statistically significant. Notably, a pectin supplement in the minimal medium significantly increased the wild type biomass by 58% but decreased the mutant biomass by 11%. The mutant grew significantly less than the wild type ($p$=0.0012, $df$ = 3) with pectin as the major carbon source.

**Expression and localization of AbVf19 protein**

To survey the expression and localization of the AbVf19 protein, we tagged its gene at the C-terminus right before the stop codon with a *GFP* coding sequence (Lorang et al., 2001). The tagging construct was designed for the GFP protein to be expressed as a fusion protein with an AbVf19 gene that was regulated by its native enhancer and promoter elements. As a negative control, we also made mutants that expressed GFP with a constitutive *ToxA* promoter (Ciuffetti et al., 1997b). All GFP signals in the negative control mutant stayed in the cytoplasm and never

located in the nuclei (Fig. 6 A). In contrast, the GFP signals were located in the nuclei of the mutant expressing AbVf19-GFP fusion proteins (Fig 6, B-F). The AbVf19-GFP protein was expressed in all fungal tissues during all stages of host infection from 24 to 96 hpi. The AbVf19-GFP protein was also expressed in hyphae during growth in axenic media, although it was expressed at a lower level than during plant infection.

**Downstream genes regulated by *AbVf19***

To study the regulatory roles of *AbVf19* in *A. brassicicola*, we compared gene expression profiles between the wild type and the *Δabvf19* mutant at 96 hpi, the late stage of infection. We inoculated nine detached leaves harvested from three plants with conidia from the *Δabvf19* mutant and the wild type. Tissue samples containing both host plant tissue and fungal hyphae were harvested. Three biological replicates were prepared for the mutant and three for the wild type and their gene expression profiles compared.

A total 27 and 74 genes among *A. brassicicola*'s 10,688 predicted genes were significantly up- or down-regulated, respectively, more than 2-fold ($p<0.05$) in the *Δabvf19* mutant compared to the wild type (Supp. Table 1). This respectively represents 0.25% and 0.69% of the genes in the *A. brassicicola* genome. Functional categories that were overrepresented in the down-regulated genes included 15 glycoside hydrolases, 6 pectate lyases, and 6 peptidases (Supp. Table 2). In addition, one of 9 cutinases was also down-regulated 73-times. We examined the reliability of the gene expression data produced by RNA-seq by quantitative real time PCR (qRT-PCR) with two differentially expressed genes and one non-differentially expressed genes. They showed comparable results to the RNA-seq data (Supp. Fig. 2).

**Conserved sequence motifs shared among downstream genes**

In order to discover common motifs at the putative promoter region among down-regulated genes in the mutants, we surveyed the putative promoter regions of the genes with expression values over 300 mapped Fragments Per Kilobase of exon model per Million (FPKM) in the wild type *A. brassicicola* and below 100 FPKM in *Δabvf19*. There were nine genes that matched these criteria. Comparison of the promoters of these genes revealed a conserved motif shared by all nine genes (Fig. 7). Next, occurrences of the same motif were counted within the promoter

regions of 56 other down-regulated genes in the mutant. Of the 56 genes, 17 had at least 1 conserved motif in their promoter region. The frequency of this motif among the 56 genes is significantly greater than can be randomly selected from the pool of 1071 promoters with the motif among a total of 8247 promoters ($p = 5x10^{-4}$). The motif showed similarity to the previously described binding site of a zinc finger transcription factor in the JASPAR CORE database (MA0036.1, $p = 4x10^{-3}$) and contains a GATA submotif characteristic of zinc finger transcription factors. The cutinase encoding gene *CutAb* that was expressed 73-times more in the wild type than in the mutant had two binding motifs while the other eight cutinase genes did not have the same motif.

**Plant responses**

The sequence tags used to identify differentially expressed genes in the Δ*abvf19* mutant and wild type *A. brassicicola* were also aligned to 14,000 full-length cDNA sequences of *B. oleracea*. Several putative defense-related genes were highly expressed in plants that were inoculated with either the wild type or the mutant. They are lectin domain-containing protein, pathogenesis-related protein 1, reticulin oxidase-like protein, psi-producing oxygenase, cytochrome P450, and D-glucan cellobiohydrolase. However, no plant genes were differentially expressed during the challenge by the wild type and the *Δabvf19* mutant.

**Reduced virulence in *Arabidopsis* PAD3 mutants**

Gene expression profiles at a late stage of infection suggested that the reason for the decrease in virulence of Δ*abvf19* was the reduced expression of several enzymes putatively important for depolymerization of plant material. To further test the effects of a lack of phytoalexin and the delayed response of plant resistance (PR) genes on the severity of the mutant's virulence, we compared the virulence of the *Δabvf19* mutants on wild type of *Arabidopsis thaliana* (Columbia ecotype) and its *pad3* mutant. The *pad3* mutant does not produce the phytoalexin, Camalexin, and is more susceptible to *Alternaria brassicicola* (Narusaka et al., 2003; Zhou et al., 1999). The *Δabvf19* mutant was expected to be more virulent on the *pad3* mutant than on the Columbia ecotype if the *Δabvf19* mutant could not detoxify Camalexin. The *Δabvf19* mutant failed to cause lesions or were only weakly virulent on *pad3* plants (Fig. 8).

## DISCUSSION

Multiple strains of disruption and deletion mutants of the *AbVf19* gene consistently displayed a ~90% reduction in virulence compared to wild-type *A. brassicicola*. The reduced virulence was restored by complementing a *Δabvf19* mutant with the wild-type allele of its AbVf19 gene. These pathogenicity assay results showed that the severe reduction of virulence in the mutants was due to the loss of the *AbVf19* gene functions.

The predicted amino acid sequence of the AbVf19 protein contains nuclear localization signals and tandem $C_2H_2$- zinc finger domains (Pfam ID: PF00096) (Bateman et al., 2004). The nuclear localization of AbVf19 protein was confirmed by accumulated green fluorescence signals from AbVf19-GFP fusion proteins. The $C_2H_2$-zinc finger is best known for its binding in the major groove of DNA and is typically spaced at 3-bp intervals. The α-helix expanding two conserved histidines in each domain can make sequence-specific contacts to DNA bases (Iuchi, 2001). Residues from a single helix can contact four or more bases, producing an overlapping pattern of contacts with adjacent zinc fingers. The accumulation of AbVf19 proteins in nuclei and the presence of DNA-binding motifs in the predicted amino acid sequence indicated that AbVf19 is a transcription factor.

### Mechanisms of reduced virulence in the *Δabvf19* mutant

The Δ*abvf19* mutant expressed fewer transcripts for 74 genes than wild-type *A. brassicicola* during the late stage of infection. Among these 74 down-regulated genes several hydrolytic enzyme genes were over-represented. Their predicted functions suggested depolymerization of cell wall components or extracellular proteins. Although we cannot rule out the possible importance of other genes, they included neither peroxysomal enzymes such as catalases or dismutases, nor detoxification enzymes such as glucosyltransferase genes (Sexton et al., 2009) and dithiocarbamate hydrolase (Pedras et al., 2009b). The gene expression study suggested that inefficient detoxification of reactive oxygen species or phytoalexins in the host plant was not the main cause for the decrease in Δ*abvf19* mutant virulence. In addition, mutant growth was not affected by the presence of reactive oxygen *in vitro* and mutants were equally less virulent in phytoalexin-deficient host plants. The results of gene expression studies and *in vitro* growth

assays consistently suggested that the reduced expression of 26 hydrolytic enzymes (putative CWDEs and proteases) were the major reason for the ~90% reduction in mutant virulence.

Plant infection by fungi is characterized by the catabolism of internal lipid stores in the early stage and by the use of readily available external sugars and amino acids during the middle stage (Reviewed in (Solomon et al., 2003), reference sugar transport). Relatively little is known about the major nutrient sources of fungal metabolism during the late stage of infection. The regulation of CWDE expression is orchestrated by sucrose nonfermenting 1 (SNF1) homologs in two distantly related fungi (Ospina-Giraldo et al., 2003; Tonukari et al., 2000). A kinase *ccSNF1* in *Cochliobolus carbonum* regulates a suite of CWDE genes during pathogenesis. Its mutants were less able to digest the main components of host plant cell walls and had a severe reduction in virulence. The primary role of genes regulated by *ccSNFI* was in the penetration of host leaves, however, not in utilization of plant materials as nutrients. Unlike Δ*ccsnf1* mutants, the Δ*abvf19* mutant was similar to wild-type *A. brassicicola* in its appressorium-like structure formation and penetration. The main difference is in the much smaller lesions caused by mutants compared to the wild type.

**Specialized hydrolytic enzyme genes for pathogenesis**

Hydrolytic enzyme-coding genes with reduced expression in the mutant during late infection represented only a few genes within each gene family. For example, only 1 of 9 cutinase genes, 15 of 171 glycoside hydrolase genes, 6 of 235 peptidases, and 5 of 18 pectate lyase genes, were down-regulated in the mutant during late-stage infection (Table 2). The vegetative growth rate of the mutant was similar to the wild type in an axenic broth medium containing either glucose as a major carbon source or yeast extract as a major nitrogen source (Fig. 4). This result suggested that *AbVf19* and its downstream hydrolytic enzyme genes were not associated with utilization of these nutrients derived from non-host plants. We speculate that these differentially expressed genes encode proteins important in depolymerizing plant substrates for use as nutrients. The importance of enzymes in depolymerizing host plant materials in late-stage pathogenesis was proposed previously (Solomon et al., 2003). Some hydrolytic enzymes are dominantly expressed during late-stage infection in other phytopathogenic fungi (Dean et al., 2005; Hane et al., 2007).

Our experimental evidence suggested that *AbVf19* regulated only a small number of genes within each family of enzyme-coding genes and that these genes are important for successful infection.

**Importance of a coordinated expression of individual genes**

Down-regulated genes in the Δ*abvf19* mutant included *Cbh7* and a chymotrypsin-coding gene that showed 21- and 2.6-times fewer transcripts than wild-type *A. brassicicola*. These genes were known to be induced during pathogenesis (Cho et al., 2007; Cramer et al., 2006; Lev and Horwitz, 2003). They were considered important for pathogenesis based on their highly elevated expression level. Mutation of the chymotrypsin-coding gene or *Cbh7*, however, did not lead to a significant reduction in virulence (Cho, unpublished data). Similarly, the cutinase gene (*CutAb*) had 73-times fewer transcript in the Δ*abvf19* mutant in this study, but *cutab* mutants in Yao and Köller's did not affect virulence (Yao and Köller, 1995). These mutation studies suggested that each enzyme-coding gene either contributed little to virulence, or their functions were redundant as proposed previously based on *ccSNF1* and *foSNF1* studies (Ospina-Giraldo et al., 2003; Tonukari et al., 2000). The current Δ*abvf19* mutant study supports the importance of coordinated regulation of those genes during pathogenesis.

**Mechanistic roles of AbVf19**

The AbVf19 protein was consistently localized in wild-type *A. brassicicola* during plant infection and during saprophytic growth in axenic media. Deletion of this gene, however, affected only the pathogenicity, but not saprophytic growth in axenic media containing nutrients derived from non-host plants. These two contrasting results suggested that the regulatory functions of the AbVf19 depended on either modification of AbVf19 or the presence of cofactors. The transcription factor binding motif (Fig. 7) was compatible with cutinase expression data. Only one of nine genes in the family have a putative *cis*-element shared among down-regulated genes and its expression level was 73-times lower in the mutant than in the wild type. The other eight cutinase genes did not have the binding motif and were not differentially expressed. However, the same binding site was not compatible with pectate lyase expression. We could not find a correlation between the presence and absence of the binding site and the differential expression of pectate lyase. The AbVf19 proteins might have required additional transcription factors (cofactors) and each co-factor acted as a determinant for the regulation of

downstream genes. Many hydrolytic enzymes are sequentially induced in *A. brassicicola* during pathogenesis (Fan and Köller, 1998; Thomma, 2003). The AbVf19 proteins may be involved in sequential regulation of a gamut of genes with the aid of various co-transcription factors. Regardless the nature of the regulation mechanisms of AbVF19, its amino acid sequence is highly conserved among *Alternaria spp*. but highly diverged from animal transcription factors. It is a potential target for the control *Alternaria spp.* with minimal impacts on animals.

## MATERIALS AND METHODS

### Transformation and maintenance of fungal strains

We used the facultative plant pathogen *Alternaria brassicicola* (ATCC96836) in this study. Growth and maintenance of the fungus and its transformation, nucleic acid isolation, mutant purification, and mutant verification by Southern hybridization were performed as described previously (Cho et al., 2009). The wild-type fungus and each of the mutant strains created during this study were purified by two rounds of single-spore isolation to obtain a more uniform genetic background. The cultures were maintained as glycerol stock in separate tubes with one tube used for each assay. Primers used in this study are listed in Supplementary Table 1.

### Determination of the full-length sequence

Using the partial sequence of the AbVf19 gene in the draft genome sequence (http://jgi.doe.gov/Abrassicicola), we designed one primer, AbVf19Fseq (tacatcgacgacaactgc), in the coding region of the gene at the end of the contig. Another primer, AbVf19Rseq (ggattgagcagactcgaagc), was designed at the adjacent contig. These two primers were used to amplify the gap between the two contigs. The PCR products were used as template DNA and the sequence was determined with the two PCR primers.

### Gene phylogeny

The predicted amino acid sequence of AbVf19 was used as a query for Blast search against the NCBI database. The sequence alignment file was exported as a fasta format from NCBI and manually refined using the MEGA 5 suite (Tamura et al., 2007). All fungi were constrained in

four major fungal groups before phylogenetic analysis. The MP tree was obtained using the Min-mini heuristic algorithm (pg. 128 in ref. (Nei and Kumar, 2000)) with a search factor of 3. The analysis involved 37 amino acid sequences. All positions with less than 50% site coverage were eliminated. That is, fewer than 50% alignment gaps, missing data, and ambiguous bases were allowed at any position. There were a total of 611 positions in the final dataset. Evolutionary analyses were conducted in MEGA5. GenBank accession numbers for all taxa were listed in Supplementary Table 3.

**Generation of deletion mutants for *AbVf19***

All transformation constructs described in this work were produced by a double-joint PCR method (Yu et al., 2004) with modifications described previously (Cho et al., 2009). We made *AbVf19* deletion mutants by replacing the gene with a HygB cassette. The replacement construct was produced with the following three sets of primers. The primer set 1zAbVf19-5F (tagctgtcttttcggccact) and 2HygFcZAbVf19-5R (atcagttaacgtcgacctcgcaaagagtgtgagggcacaa), and the primer set 5HygRcZAbVf19-3F (ggaaccagttaacgtcgacgcgagattggcattttggttt) and 6z9219-3R (cttccaggacgcttctcaac) were used respectively to amplify the 5' and 3' flanking regions of the targeted locus. Another set of primers, 3zAbVf19-5RcHygF (ttgtgccctcacactctttgcgaggtcgacgttaactgat) and 4zAbVf19-3FcHygR (aaaccaaaatgccaatctcgcgtcgacgttaactggttcc), was used to amplify the HygB-selectable marker gene cassette (1,436 bp) from pCB1636. The final transformation constructs were produced by PCR amplification using the mix of products from three reactions as template DNA and two primers, 1zAbVf19-5F and 6z9219-3R.

**Generation of mutants expressing *AbVf19-GFP* fusion proteins**

In order to create mutants expressing green fluorescence protein fused to the C-terminal of AbVf19, the *AbVf19* coding region (1,209 bp) and 3' flanking region (192 bp) were amplified with zAbVf19ProbeF (gccattaactccgtcacgtt) and 2zAbVf19GFP-GA (accatggcaccggctccagcgcctgcaccagctcccctcttacgcttcttctggcta), and 5HygRcZAbVf19-3F (ggaaccagttaacgtcgacgcgagattggcattttggttt) and 6'z9219-3R (acgagtgtaggaagcgcaag), respectively. Another set of primers, 3zAbVf195FPF-GA (gtaagaggggagctggtgcaggcgctggagccggtgccatggtgagcaagggcgag) and 4zAbVf19-3FcHygR

(aaaccaaaatgccaatctcgcgtcgacgttaactggttcc), was used to amplify the 2,384 bp that covered the coding regions of the GFP and the HygB cassette. The final transformation constructs were produced by PCR amplification from the mixture of the PCR products using zAbVf19ProbeF and 6'z9219-3R.

**Complementation of the *Δabvf19* mutants**

The *Δabvf19* mutant was complemented with the wild-type *AbVf19* allele with its native promoter. We used two primers to reintroduce wild-type *AbVf19* into the *Δabvf19-8* mutant, 1zAbVf19-5F and 6z9219-3R. These primers amplified the 4,200 bp wild-type allele of the *AbVf19* gene using *A. brassicicola* genomic DNA as a template. The PCR product included a 1,223 bp 5' flanking region, 1,747 bp complete coding region, and a 1,230 bp 3' flanking region. Separately, pNR-20F (aaagggaacaaaagctggag) and pNR-775R (cctcgaggtcgacggtatc) were used to amplify a 2,226 bp-long nourseothricin-resistant cassette as a selectable marker gene, using a pNR vector as the template(Malonek et al., 2004). These two products (7 µg of *AbVf19* and 3 µg of *NTC* cassette) were mixed to transform the *Δamr1* mutant. Complemented mutant clones were purified by two rounds of single-spore isolation.

**Pathogenicity assays**

Pathogenicity assays were performed on either whole plants or detached leaves harvested from 5-to-8-week-old green cabbage (*Brassica oleracea*) plants or *Arabidopsis thaliana*. *Arabidopsis thaliana* plants included the Columbia ecotype and its *pad3* mutant (Zhou et al., 1999). For most detached leaf assays, leaves were removed, placed in mini-moist chambers, and randomly located on a laboratory bench. For the pathogenicity assays on whole plants, potted plants were placed in a semi-transparent plastic trough with adequate water. The troughs with plants inside were sealed with saran wrap after inoculation to keep the relative humidity close to 100%. The decreased virulence of each mutant was calculated using the formula $(\sum(Dwi\text{-}Dmi)/ \sum(Dwi)) \times 100$, where Dw*i* was the lesion diameter created by the wild-type for the *i*th sample and Dm*i* was the lesion diameter produced by the mutant for the *i*th sample.

**Confocal Microscopy**

Infected plant tissues were trimmed with a razor blade, placed on microscope slides, and covered with Gold Seal cover glasses. Confocal images were acquired using a 633 C-Apochromat (numerical aperture 1.2) water-immersion objective lens and an Olympus Fluoview 1000 Laser Scanning Confocal System on a IX-81 inverted microscope. Spectra for fungal tissues expressing standard green fluorescence and for plant cells emitting autofluorescence were collected by simultaneous 488 nm and 543 nm excitation using 30 mW argon and 1 mW helium:neon lasers, respectively. The standard GFP spectrum was collected through 488 nm excitation using a 20 nm window from 505 to 525 nm. Plant tissue, including chloroplasts, was visualized using a 543 nm excitation with a 560 nm-long pass filter. Images of fungal tissue grown in nutrient media were captured with 488 nm excitation and DIC-transmitted light. All fluorescent images were composed of multiple layers acquired with the Confocal System.

**Salt or oxygen stress tests**

Each fungal strain from glycerol stocks was inoculated on PDA with an appropriate selectable marker and grown in the dark for 5 days at 25˚C. In order to test for sensitivity to osmotic stress and oxygen radicals, wild-type and mutant conidia were pipetted onto PDA containing 2% (w/v) or 4% (w/v) NaCl, 2.5 mM or 5 mM $H_2O_2$, or 2 mM or 4 mM $KO_2$. Colony diameters were measured 4 days post-inoculation (dpi). The experiment was conducted three times.

**Synthetic media and vegetative growth assays**

We made a minimal medium broth containing 0.5% $(NH_4)_2SO_4$, 0.05% yeast extract, salts (0.15% $KH_2PO_4$, 0.06% $MgSO_4$, and 0.06% $CaCl_2$), and trace amounts of metals (0.0005% $FeSO_4$ $7H_2O$, 0.00016% $MnSO_4$ $H_2O$, 0.00014% $ZnSO_4$ $7H_2O$, and 0.00037% $CoCl_2$). Agar powder was added to the minimal medium broth to make minimal medium agar (2% (w/v)). The agar was supplemented with a carbon source as described. Flasks (250 ml) containing a 50 ml minimal medium broth were supplemented with either 1% glucose or 1% of another complex carbon source, such as α-cellulose, xylan, or citrus pectin (Sigma, St. Louis, MO). Each flask was inoculated with 5 x $10^5$ conidia of either the *Δabvf19* mutant or the wild type. The flasks were incubated in the dark at 25°C with continuous agitation at 100 rpm. Mycelia were harvested at 4 dpi, washed with distilled water, and dried at 105°C overnight. The decreased biomass of each mutant and wild type was calculated using the formula $(\sum(Ww_i\text{-}Wm_i)/ \sum(Ww_i))$

x 100, where Ww*i* was the dry weight of the wild type for the *i*th sample and Wm*i* was the weight of the mutant for the *i*th sample.

**RNAseq gene expression analysis**

The sequenced reads were mapped to the genome sequence of *A. brassicicola* (http://jgi.doe.gov/Abrassicicola) and the UniGene sequences of *B. oleracea* (ftp://ftp.ncbi.nih.gov/repository/UniGene/Brassica_oleracea/) using the program Tophat 1.3.1 (Trapnell et al., 2009) and Bowtie 0.12.7 (Langmead et al., 2009). Default settings were used, with these exceptions: the segment length was set at 20 nucleotides and the number of allowed segment mismatches was set at 1 nucleotide. Additionally, intron length was designated as a minimum of 10 nucleotides and a maximum of 400 nucleotides. The program Cuffdiff version 1.0.3 (which is part of Cufflinks, (Trapnell et al., 2010)) was used to identify reads overlapping with previously predicted genes. The expression levels of each predicted gene were determined and normalized by the mapped Fragments Per Kilobase of exon model per Million (FPKM). Differentially expressed genes between the wild type and the mutant were determined by comparing FPKM from three biological replicates for both the wild type and the mutant. We also applied a cutoff of at least a two-fold change in expression value for differential expression. The bias correction method was used while running Cuffdiff (Roberts et al., 2011). Custom scripts were written in Python to analyze the data.

**Representation analysis**

Custom scripts were developed in Python and R to analyze over- and under-representation of functional annotation terms in sets of differentially regulated genes using the Fisher Exact test. The Benjamini-Hochberg correction was used to correct for multiple testing using a *p*-value of 0.05.

**Identification of transcription factor binding sites**

MEME Suite 4.5.0 (Bailey and Elkan, 1994) was used to identify conserved motifs in the promoters of genes. Promoters are defined here as the nucleotide sequence 750 bp upstream of the translation start site of predicted genes. Incomplete promoters (with less than 750 bp of available sequence or containing gaps) were excluded from the analysis. Parameters were

chosen to identify conserved motifs of up to 10 nucleotides, with zero or one expected occurrence in each promoter on both strands. The nucleotide frequencies of all promoters were used as background frequencies. The identified motifs were manually inspected. Next, occurrences of the relevant motifs in the full promoter set were counted using FIMO, which is part of the MEME Suite. Significance of over-representation of the identified motifs in the promoter subset was determined with the Fisher Exact test. To identify the similarity of the identified motifs with previously published motifs, TOMTOM ((Gupta et al., 2007), part of the MEME Suite) was used to search the JASPAR CORE database of transcription factor-binding profiles (Bryne et al., 2008).

**Quantitative real-time PCR (Mut9619_4dpi_20110427: pec, cbh7, chymo, actin)**

The *Δabvf19* mutant and wild type were used for qRT-PCR. Two micrograms of total RNA were transcribed to cDNA in a final volume of 20 µl using 50 ng of random pentamers and 200 ng of poly$(T)_{20}$N with Superscript III (Invitrogen, Carlsbad, CA). Each cDNA was diluted 1:20. Subsequent qRT-PCR reactions were performed in a 20 µl volume containing 120 nM of each primer, 1 µl of diluted cDNA, and 10 µl of FastStart SYBRGreen Master (Roche, Mannheim, Germany). Each reaction was run in triplicate in a Biorad I-cycler (Bio-Rad, Hercules, CA, USA) as described previously (Cho et al, 2006). Relative amounts of the transcript of each gene were calculated as $2^{-\Delta Ct}$ using a threshold cycle (Ct), where $\Delta Ct = (Ct_{,gene\,i} - Ct_{,actin})$. Fold changes of each gene between the wild type and *Δamr1* strain were calculated as $2^{-\Delta\Delta Ct,}$ where $\Delta\Delta Ct = (Ct_{,gene\,i} - Ct_{,actin})_{\Delta amr1} - (Ct_{,gene\,i} - Ct_{,actin})_{wild\ type}$.

**ACKNOWLEDGEMENTS**

We thank Tina M. Carvalho, Wayne Borth, Ann Alvarez, and John Hu for generously sharing their research equipment. This research was supported by USDA-TSTAR 2009-34135-20197 and HATCH funds to Y.C, administered by the College of Tropical Agriculture and Human Resources, University of Hawaii at Manoa, Honolulu, HI. Analysis of RNAseq data and downstream analyses were done by the U.S. Department of Energy Joint Genome Institute that is supported by the Office of Science of the U.S. Department of Energy under Contract No. DE-AC02-05CH11231

## REFERENCES


Bailey, T. L., Elkan, C., 1994. Fitting a mixture model by expectation maximization to discover motifs in biopolymers. Proc. Int. Conf. Intell. Syst. Mol. Biol. 2**,** 28-36.

Bateman, A., Coin, L., Durbin, R., Finn, R. D., Hollich, V., Griffiths-Jones, S., Khanna, A., Marshall, M., Moxon, S., Sonnhammer, E. L., Studholme, D. J., Yeats, C., Eddy, S. R., 2004. The Pfam protein families database. Nucleic Acids Res. 32**,** D138-41.

Bryne, J. C., Valen, E., Tang, M. H., Marstrand, T., Winther, O., da Piedade, I., Krogh, A., Lenhard, B., Sandelin, A., 2008. JASPAR, the open access database of transcription factor-binding profiles: new content and tools in the 2008 update. Nucleic Acids Res. 36**,** D102-6.

Cho, Y., Cramer, R. A., Jr., Kim, K. H., Davis, J., Mitchell, T. K., Figuli, P., Pryor, B. M., Lemasters, E., Lawrence, C. B., 2007. The Fus3/Kss1 MAP kinase homolog *Amk1* regulates the expression of genes encoding hydrolytic enzymes in *Alternaria brassicicola*. Fungal Genet Biol. 44**,** 543-53.

Cho, Y., Davis, J. W., Kim, K. H., Wang, J., Sun, Q. H., Cramer, R. A. J., Lawrence, C. B., 2006. A high throughput targeted gene disruption method for *Alternaria brassicicola* functional genomics using linear minimal element (LME) constructs. Mol Plant Microbe Interact. 19**,** 7-15.

Cho, Y., Kim, K.-H., La Rota, M., Scott, D., Santopietro, G., Callihan, M., Lawrence, C. B., 2009. Identification of virulence factors by high throughput targeted gene deletion of regulatory genes in *Alternaria brassicicola*. Mol. Microbiol. 72**,** 1316 - 1333.

Churchill, A., LU, S., Turgeon, B., Yoder, O., Macko, V., 1995. Victorin-deficient REMI mutants of *Cochliobolus victoriae* demonstrate a requirement for victorin in pathogenesis. Fung. Genet. Newslett. 42A**,** 41.

Ciuffetti, L., Tuori, R., Gaventa, J., 1997a. A single gene encodes a selective toxin causal to the development of tan spot of wheat. Plant Cell. 9**,** 135-144.

Ciuffetti, L. M., Tuori, R. P., Gaventa, J. M., 1997b. A single gene encodes a selective toxin causal to the development of tan spot of wheat. Plant Cell. 9**,** 135-44.

Cramer, R. A., La Rota, C. M., Cho, Y., Thon, M., Craven, K. D., Knudson, D. L., Mitchell, T. K., Lawrence, C. B., 2006. Bioinformatic analysis of expressed sequence tags derived from a compatible *Alternaria brassicicola-Brassica oleracea* interaction. Molecular Plant Pathology. 7**,** 113-124.

Dean, R. A., Talbot, N. J., Ebbole, D. J., Farman, M. L., Mitchell, T. K., Orbach, M. J., Thon, M., Kulkarni, R., Xu, J. R., Pan, H., Read, N. D., Lee, Y. H., Carbone, I., Brown, D., Oh, Y. Y., Donofrio, N., Jeong, J. S., Soanes, D. M., Djonovic, S., Kolomiets, E., Rehmeyer, C., Li, W., Harding, M., Kim, S., Lebrun, M. H., Bohnert, H., Coughlan, S., Butler, J., Calvo, S., Ma, L. J., Nicol, R., Purcell, S., Nusbaum, C., Galagan, J. E., Birren, B. W., 2005. The genome sequence of the rice blast fungus *Magnaporthe grisea*. Nature. 434**,** 980-6.

Del Sorbo, G., Scala, F., Parrella, G., Lorito, M., Comparini, C., Ruocco, M., Scala, A., 2000. Functional expression of the gene cu, encoding the phytotoxic hydrophobin cerato-ulmin, enables *Ophiostoma quercus*, a nonpathogen on elm, to cause symptoms of Dutch elm disease. Mol Plant Microbe Interact. 13**,** 43-53.

Fan, C.-Y., Köller, W., 1998. Diversity of cutinases from plant pathogenic fungi: differential and sequential expression of cutinolytic esterases by *Alternaria brassicicola*. FEMS Microbiology Letters. 158**,** 33-38.

Gu, Z., Nicolae, D., Lu, H. H., Li, W. H., 2002. Rapid divergence in expression between duplicate genes inferred from microarray data. Trends Genet. 18**,** 609-13.

Gupta, S., Stamatoyannopoulos, J. A., Bailey, T. L., Noble, W. S., 2007. Quantifying similarity between motifs. Genome Biol. 8**,** R24.

Hane, J. K., Lowe, R. G., Solomon, P. S., Tan, K. C., Schoch, C. L., Spatafora, J. W., Crous, P. W., Kodira, C., Birren, B. W., Galagan, J. E., Torriani, S. F., McDonald, B. A., Oliver, R. P., 2007. Dothideomycete plant interactions illuminated by genome sequencing and EST analysis of the wheat pathogen *Stagonospora nodorum*. Plant Cell. 19**,** 3347-68.

Hashimoto, M., Higuchi, Y., Takahashi, S., Osada, H., Sakaki, T., Toyomasu, T., Sassa, T., Kato, N., Dairi, T., 2009. Functional analyses of cytochrome P450 genes responsible for the early steps of brassicicene C biosynthesis. Bioorg Med Chem Lett. 19**,** 5640-5643.

Horton, P., Nakai, K., 1997. Better prediction of protein cellular localization sites with the k nearest neighbors classifier. Proc Int Conf Intell Syst Mol Biol. 5**,** 147-52.

Ito, K., Tanaka, T., Hatta, R., Yamamoto, M., Akimitsu, K., Tsuge, T., 2004. Dissection of the host range of the fungal plant pathogen *Alternaria alternata* by modification of secondary metabolism. Mol Microbiol. 52**,** 399-411.

Iuchi, S., 2001. Three classes of C2H2 zinc finger proteins. Cell Mol Life Sci. 58**,** 625-35.

Johnson, R. D., Johnson, L., Itoh, Y., Kodama, M., Otani, H., Kohmoto, K., 2000. Cloning and characterization of a cyclic peptide synthetase gene from *Alternaria alternata* apple pathotype whose product is involved in AM-toxin synthesis and pathogenicity. Mol Plant Microbe Interact. 13**,** 742-53.

Langmead, B., Trapnell, C., Pop, M., Salzberg, S. L., 2009. Ultrafast and memory-efficient alignment of short DNA sequences to the human genome. Genome Biol. 10**,** R25.

Lev, S., Horwitz, B. A., 2003. A mitogen-activated protein kinase pathway modulates the expression of two cellulase genes in *Cochliobolus heterostrophus* during plant infection. Plant Cell. 15**,** 835-844.

Lorang, J. M., Tuori, R. P., Martinez, J. P., Sawyer, T. L., Redman, R. S., Rollins, J. A., Wolpert, T. J., Johnson, K. B., Rodriguez, R. J., Dickman, M. B., Ciuffetti, L. M., 2001. Green fluorescent protein is lighting up fungal biology. Appl Environ Microbiol. 67**,** 1987-94.

Malonek, S., Rojas, M. C., Hedden, P., Gaskin, P., Hopkins, P., Tudzynski, B., 2004. The NADPH-cytochrome P450 reductase gene from *Gibberella fujikuroi* is essential for gibberellin biosynthesis. J Biol Chem. 279**,** 25075-84.

Narusaka, Y., Narusaka, M., Seki, M., Ishida, J., Nakashima, M., Kamiya, A., Enju, A., Sakurai, T., Satoh, M., Kobayashi, M., Tosa, Y., Park, P., Shinozaki, K., 2003. The cDNA microarray analysis using an Arabidopsis pad3 mutant reveals the expression profiles and classification of genes induced by *Alternaria brassicicola* attack. Plant Cell Physiol. 44**,** 377-87.

Nei, M., Kumar, S., 2000. Molecular Evolution and Phylogenetics. Oxford University Press, New York.

Oka, K., Akamatsub, H., Kodamab, M., Nakajimab, H., Kawadab, T., Otani, H., 2005. Host-specific AB-toxin production by germinating spores of *Alternaria brassicicola* is induced by a host-derived oligosaccharide. Physiological and Molecular Plant Pathology. 66**,** 12-19.

Ospina-Giraldo, M. D., Mullins, E., Kang, S., 2003. Loss of function of the *Fusarium oxysporum* SNF1 gene reduces virulence on cabbage and *Arabidopsis*. Curr Genet. 44**,** 49-57.

Otani, H., Kohnobe, A., Kodama, M., Kohmoto, K., 1998. Production of a host-specific toxin by germinating spores of *Alternaria brassicicola*. Physiological and Molecular Plant Pathology. 52**,** 285-295.

Pedras, M. S., Chumala, P. B., Jin, W., Islam, M. S., Hauck, D. W., 2009a. The phytopathogenic fungus Alternaria brassicicola: phytotoxin production and phytoalexin elicitation. Phytochemistry. 70**,** 394-402.

Pedras, M. S., Minic, Z., Sarma-Mamillapalle, V. K., 2009b. Substrate specificity and inhibition of brassinin hydrolases, detoxifying enzymes from the plant pathogens Leptosphaeria maculans and Alternaria brassicicola. FEBS J. 276**,** 7412-28.

Roberts, A., Trapnell, C., Donaghey, J., Rinn, J. L., Pachter, L., 2011. Improving RNA-Seq expression estimates by correcting for fragment bias. Genome Biol. 12**,** R22.

Seidl, V., Seiboth, B., Karaffa, L., Kubicek, C. P., 2004. The fungal STRE-element-binding protein *Seb1* is involved but not essential for glycerol dehydrogenase (*gld1*) gene expression and glycerol accumulation in *Trichoderma atroviride* during osmotic stress. Fungal Genet Biol. 41**,** 1132-40.

Sexton, A. C., Minic, Z., Cozijnsen, A. J., Pedras, M. S., Howlett, B. J., 2009. Cloning, purification and characterisation of brassinin glucosyltransferase, a phytoalexin-detoxifying enzyme from the plant pathogen *Sclerotinia sclerotiorum*. Fungal Genet Biol. 46**,** 201-9.

Solomon, P. S., Tan, K. C., Oliver, R. P., 2003. The nutrient supply of pathogenic fungi; a fertile field for study. Mol Plant Pathol. 4**,** 203-10.

Spassieva, S. D., Markham, J. E., Hille, J., 2002. The plant disease resistance gene *Asc-1* prevents disruption of sphingolipid metabolism during AAL-toxin-induced programmed cell death. Plant J. 32**,** 561-72.

Tamura, K., Dudley, J., Nei, M., Kumar, S., 2007. MEGA4: Molecular Evolutionary Genetics Analysis (MEGA) software version 4.0. Mol Biol Evol. 24**,** 1596-9.

Tanaka, A., Shiotani, H., Yamamoto, M., Tsuge, T., 1999. Insertional mutagenesis and cloning of the genes required for biosynthesis of the host-specific AK-toxin in the Japanese pear pathotype of *Alternaria alternata*. Mol Plant Microbe Interact. 12**,** 691-702.

Thomma, B. P. H. J., 2003. *Alternaria* spp.: from general saprophyte to specific parasite. Molecular Plant Pathology. 4**,** 225-236.

Tonukari, N. J., Scott-Craig, J. S., Walton, J. D., 2000. The *Cochliobolus carbonum* SNF1 gene is required for cell wall-degrading enzyme expression and virulence on maize. Plant Cell. 12**,** 237-48.

Trapnell, C., Pachter, L., Salzberg, S. L., 2009. TopHat: discovering splice junctions with RNA-Seq. Bioinformatics. 25**,** 1105-11.

Trapnell, C., Williams, B. A., Pertea, G., Mortazavi, A., Kwan, G., Van Baren, M. J., Salzberg, S. L., Wold, B. J., Pachter, L., 2010. Transcript assembly and quantification by RNA-Seq reveals unannotated transcripts and isoform switching during cell differentiation. Nature Biotechnology. 28**,** 511-515.

Wagner, A., 2000. Decoupled evolution of coding region and mRNA expression patterns after gene duplication: implications for the neutralist-selectionist debate. Proc Natl Acad Sci U S A. 97**,** 6579-84.

Wight, W. D., Kim, K. H., Lawrence, C. B., Walton, J. D., 2009. Biosynthesis and role in virulence of the histone deacetylase inhibitor depudecin from *Alternaria brassicicola*. Mol Plant Microbe Interact. 22**,** 1258-67.

Yao, C., Köller, W., 1995. Diversity of cutinases from plant pathogenic fungi: different cutinases are expressed during saprophytic and pathogenic stages of *Alternaria brassicicola*. Molecular Plant-Microbe Interactions. 8**,** 122-130.

Yu, J. H., Hamari, Z., Han, K. H., Seo, J. A., Reyes-Dominguez, Y., Scazzocchio, C., 2004. Double-joint PCR: a PCR-based molecular tool for gene manipulations in filamentous fungi. Fungal Genet Biol. 41**,** 973-81.

Yun, S.-H., Turgeon, B., Yoder, O., 1998. REM-induced mutants of *Mycosphaerella zeae-maydis* lacking the polyketide PM-toxin are deficient in pathogenesis to corn. Physiol. Mol. Plant Pathol. 52**,** 53-66.

Zhang, J., 2003. Evolution by gene duplication: an update. Trends in Ecology & Evolution. 18**,** 292-298.

Zhou, N., Tootle, T. L., Glazebrook, J., 1999. Arabidopsis PAD3, a gene required for camalexin biosynthesis, encodes a putative cytochrome P450 monooxygenase. Plant Cell. 11**,** 2419-28.

Table 1. Decreased virulence of four strains of *Δabvf19* deletion mutants compared to wild-type *Alternaria brassicicola* in eleven pathogenicity assays.

| Mutants | Number of spores wt/mut | d.f. | Lesion size (mm) | | Virulence decrease | P |
|---|---|---|---|---|---|---|
| | | | Wild type | Mutant | | |
| *Δabvf19-1* | 1,800/1,900 | 8 | 19.6±2.6 | 4.3±3.2 | 78% | 4.0E-09 |
| *Δabvf19-1** | 2,000/2,000 | 8 | 10.4±5.3 | 0.9±0.9 | 92% | 7.0E-05 |
| *Δabvf19-8* | 2,000/2,025 | 8 | 9.2±4.6 | 2.1±3.0 | 77% | 1.0E-04 |
| *Δabvf19-9* | 2,000/2,050 | 8 | 11.1±4.5 | 5.4±3.1 | 51% | 2.0E-04 |
| *Δabvf19-10* | 2,000/2,025 | 8 | 9.4±4.5 | 1.8±1.9 | 81% | 8.0E-04 |

Abbreviations: wt = wild type, mut = mutant, d.f. = degrees of freedom, P = probability, lesion size indicates the average lesion diameter. Result marked with an asterisk (*) was from pathogenicity assays with whole plants, others were from assays with detached leaves.

Table 2. Down-regulated genes in the Δabvf19 mutant of A*lternaria brassicicola*.

| Gene function | Down regulated in mutant | Total numbers in the genome |
|---|---|---|
| Glycoside hydrolase | 14 | 171 |
| Pectate lyase | 5 | 18 |
| Pectinesterase | 1 | 4 |
| Cutinases | 1 | 9 |
| Peptidases | 6 | 235 |
| P450 | 4 | 79 |
| Ribonucleases | 2 | 19 |
| Unknown | 26 | 6,008 |
| Miscellaneous | 14 | 4317 |
| Total | 74 | 10,680 |

**FIGURE LEGENDS**

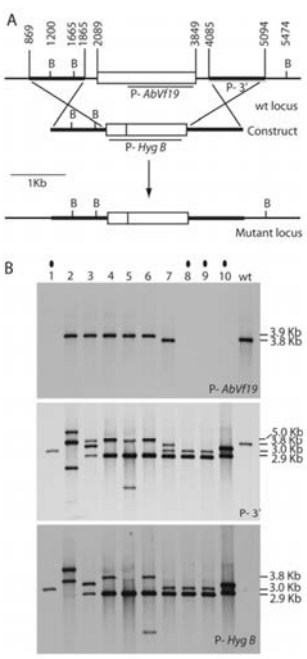


Figure 1. Deletion of the *AbVf19* gene. A. Schematic diagram of the wild-type (wt) locus, replacement construct, and mutant locus are shown in order. The mutant locus represents a scenario of replacement of the coding region of *AbVf19* gene by a single copy of a selectable marker Hygromycin B transferase (HygB) cassette. Lane 1 shows replacement of the gene by a single copy. Lanes 8, 9, and 10 show replacement of the gene by multiple copies of the replacement constructs. Dots (•) indicate DNA lanes for pathogenicity assay results presented in this study. Probe regions are marked by P-*AbVf19*, P-3', and P-*Hyg B*. Abbreviations: B = *Bam*HI enzyme digestion site.

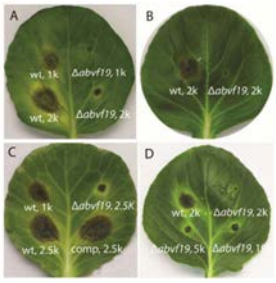


Figure 2. Decreased virulence of *Δabvf19* mutants on host plants (*Brassica oleracea*). A. Lesions on *B. oleracea* 5 days after inoculation with 1,000 or 2,000 conidia of the wild type and *Δabvf19-1* mutant on a detached leaf. B. One leaf showing lesions produced by 2,000 conidia of the wild type and *Δabvf19-1* mutant on a whole plant. The leaf was detached for photography at the end of the assay. C. Similar lesion size produced by a complemented mutant and the wild type compared to the small lesions produced by the *Δabvf19* mutant. D. Lesions produced by 2,000 conidia of the wild type (top left) and 2,000, 5,000, and 10,000 conidia of a *Δabvf19* mutant. Abbreviations: wt = wild-type *A. brassicicola*; *Δabvf19* = *AbVf19* deletion mutant; compl = mutant complemented with a native allele of the *AbVf19* gene (*Δabvf19:AbVf19*).

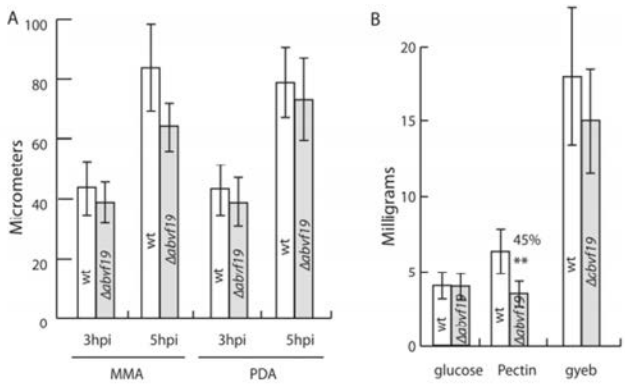


Figure 3. Comparisons of vegetative growth. A. Length of germ tubes on three different media measured at 3 and 5 hours post inoculation (hpi). B. Effect of pectin on vegetative growth of the *Δabvf19* mutant and wild type. Bars represent dry weight of mycelia in milligrams. Error bars represent standard deviation in both charts. wt = wild type, MMA = minimal media agar, PDA = potato dextrose agar, ** = ($p$<0.01).

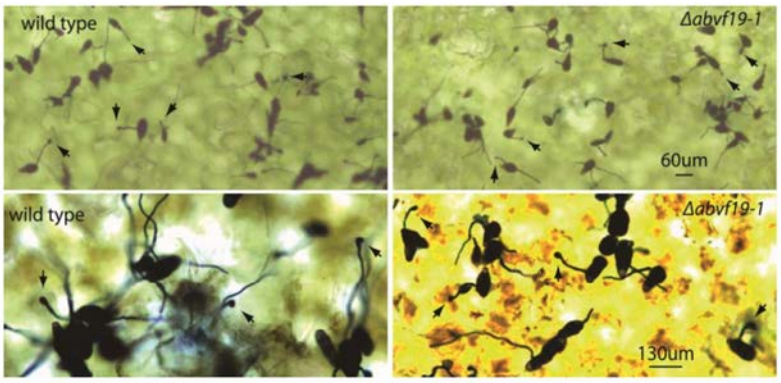


Figure 4. Germination and formation of appressorium-like structure. Images represent infection courts at 24 hours post-inoculation by the wild type (left) and *Δabvf19* mutant. Fungal tissues were stained with Trypan blue. Appressorium-like structures are marked with arrows.

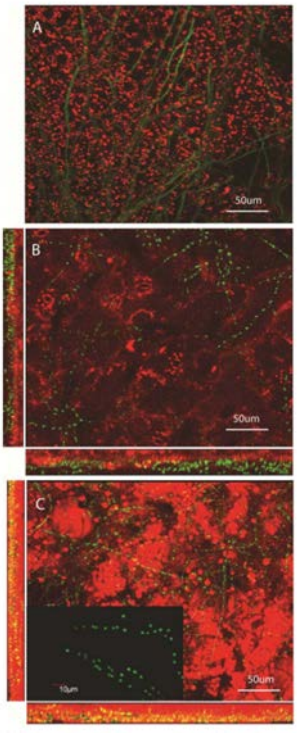


Figure 5. Confocal microscopic images showing AbVf19 protein expression and localization during pathogenesis. (rewrite)A. Composite image of green fluorescence representing AbVf19 protein and pink autofluorescence representing chloroplasts in plant tissues. Green fluorescence is weak and variable because fungal hyphae are imbedded in the plant tissues. B. GFP showing nuclei in fungal hyphae partially separated from an infected plant tissue. Green fluorescence is uniform and stronger where they are separated from the plant tissues. Scale bar = 10 µm.

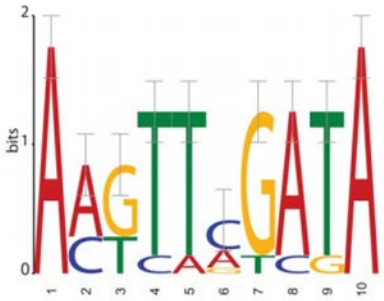


Figure 6. Putative transcription factor binding site. This motif is over-represented in promoters among the down-regulated genes in Δ*abvf19* mutants.

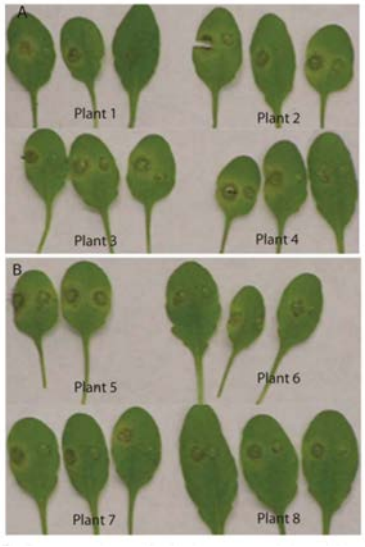


Figure 7. Decreased virulence of *Δabvf19* mutants on *Arabidopsis thaliana*. A. Lesions caused by ~2,000 conidia of the wild type and *Δabvf19-1* mutant on whole plants of the Columbia ecotype of *A. thaliana*. B. Lesions caused by the wild type and *Δabvf19-1* mutant on whole plants of the *pad3* mutant of *A. thaliana*. The leaf was detached for photography at the end of the assay. The wild type and *Δabvf19-1* mutant were inoculated on the left and right side of the leaf midvein, respectively.